

TRACING THE DYNAMICS OF THE GALACTIC DISK

Peter M. Frinchaboy

Advisor: Steven R. Majewski

Department of Astronomy, University of Virginia

Abstract

Establishing the rotation curve of the Milky Way on an absolute scale is one of the fundamental contributions needed to understand the Galaxy and its mass distribution. As preparatory work for the “Taking Measure of the Milky Way” SIM PlanetQuest Key Project, we have undertaken a systematic spectroscopic survey of open star clusters which can serve as tracers of Galactic disk dynamics. We report progress on a sample of 83 from our 100 clusters for which the Hydra multi-fiber spectrographs on the WIYN and Blanco telescopes have delivered $\sim 1 \text{ km s}^{-1}$ radial velocities (RVs) of dozens of stars per cluster. The RVs are used to derive cluster membership for individual stars in these crowded fields and to derive a bulk cluster RV. The clusters selected for study have a broad spatial distribution in order to be sensitive to the disk velocity field in all Galactic quadrants and across a Galactocentric radius range as much as 2.5 kpc from the solar circle. These clusters already have published ages, distances, and metallicity estimates, but these can be improved once chemical abundances on a uniform scale are measured from the homogeneous spectra, and once SIM PlanetQuest parallaxes are obtained for member stars. The new RVs combined with Tycho-2 proper motions (for bright members in each cluster) allow an initial investigation of the local disk dynamics, but this will be substantially improved once SIM PlanetQuest proper motions are obtained for these and even more distant open clusters.

Introduction

The NASA Space Interferometry Mission (SIM PlanetQuest) is the first space-based mission designed to obtain high quality proper motions, velocities transverse to the line of sight, and distances to stars through stellar parallax using interferometry. This mission will produce proper motions 1000 times better than its predecessor the ESA Hipparcos mission. This project is preparatory work for a SIM PlanetQuest key project, headed by Steven Majewski at the University of Virginia. The project aims to make use of the satellite’s unprecedented positional accuracy to make several definitive measurements of fundamental structural and dynamical parameters of the Milky Way (hereafter the “Galaxy”).

Because the rotation speed for stars is a function of the mass interior to the orbit, the rotation curve of a galaxy is a key method to determine its total mass and its mass dis-

tribution. The relationship between measured rotational velocity and brightness/mass in other galaxies, known as the Tully-Fisher relation, is well determined using radio astronomy. Ironically, the measurement of the rotation of the Galaxy is much more difficult for a variety of reasons, but primarily because our perspective from within the Galactic disk complicates matters considerably. First, we can no longer measure the net flow of all material, as in an external galaxy, but must instead find an appropriate type of object, a “tracer”, thought to be most characteristic of Keplerian motion. Secondly, radii no longer trivially scale by an angular distance separation from the galactic center, but now requires us to understand the much more difficult absolute distance scale. We still do not even know the solar distance to the Galactic center to better than twenty percent. Also, the rotation speed cannot necessarily be obtained by measuring a peak Doppler velocity as a function of position, as in the Tully-Fisher measures of external galaxies. Interior to the Sun’s orbit, radio astronomers can apply the “maximum velocity” tangent point method. The rotation curve is determined by measuring the peak Doppler (or radial) velocity of H I, neutral Hydrogen, in a given direction interior to the Sun’s orbit as most of the rotational velocity is in the line of sight. This is done because the distance cannot be directly found for gaseous tracers, like H I.

From our viewpoint in the Galaxy, outside the solar orbit V_{rot} is almost entirely a tangential velocity (not radial) that is much harder to measure. Therefore, V_{rot} must be determined by the measurement of both radial velocities (RV) and proper motions, velocities perpendicular to the line of sight. This requires that space-based precision proper motions need to be measured. Thus, the mass of the Galaxy has been a matter of debate for over a century. Without detailed knowledge of the Galactic rotation curve, it is difficult to tie the wealth of detailed chemodynamical data we have for the Galaxy to the global dynamics established for external galaxies. This project aims to breakthrough each of these traditional problems faced in measurement of the Galactic rotation curve.

Past analyses of Galactic rotation curve studies have various tracers, including H II regions (Fich et al. 1989), Cepheid variable stars (Pont et al. 1994), and Asymptotic Giant Branch (AGB) stars and planetary nebulae (Amaral et al. 1996), but each have shortcomings. For example, gaseous tracers (planetary nebulae and H II regions) have an inherent distance scale uncertainty; AGB stars are difficult to obtain accurate photometric distances for

in isolation, while pulsational variability complicates RV determination for Cepheids. Star clusters offer many advantages over these other tracers as compared to an isolated field star at the same location in the Galaxy, because the distance, metallicity, age, and kinematics of a cluster are much easier to establish. The 3-D kinematics of individual stars or clusters requires both proper motions and RVs, but the ability to average over an ensemble of cluster members lowers the required per star precision for the same result.

This project will derive the orbits of over 100 Galactic open clusters through use of multi-fiber spectroscopy. These data are combined with the space-based Hipparcos and Tycho-2 proper motion catalogs (Dias et al. 2001, 2002a). There have been three large surveys to determine bulk Galactic cluster proper motions as the average of the proper motion of presumed cluster stars, which have resulted in published motions for 290 total open clusters. However, a comparison of the derived motions for 101 clusters in common between the surveys reveals some discrepancy. Given the per star precisions of these catalogs, it is almost certainly the case that discrepancies compared to other work are the result of problems with identifying true cluster members, and not necessarily with the integrity of the astrometry itself. To address this problem, we have undertaken a survey to obtain precision radial velocities (RVs) to verify cluster membership for the stars used to define the cluster proper motions. The resulting very precise mean RV of each cluster, when combined with the corrected proper motions, allows us to determine the orbits of these clusters. Additionally, in the future, our radial velocities will be combined with the proper motions from SIM PlanetQuest to yield orbits of outer Galactic clusters hundreds of times better than the current project, that will be used as dynamical probes of the Galaxy’s gravitation potential. Our survey consists of clusters selected in the range of 0.3 to 3.0 kiloparsecs (kpc) from the Sun.

Observations and Data Reduction

CTIO Data

Spectroscopic data were obtained using the Hydra multiobject spectrograph on the Blanco 4-m telescope at Cerro Tololo Inter-American Observatory (CTIO). Table 1 lists the clusters observed and some of their basic properties. Data at CTIO were taken using the Hydra multiobject spectrograph and a 2048×4096 pixel CCD (SITE400mm) on the nights of 2002 March 8–12, 2003 March 16–21, 2003 July 20–23, and 2003 August 2–8 (Runs 1, 2, 3, and 4). The data were taken using the 380 grating and the $100\mu\text{m}$ slit plate, yielding a dispersion of 0.68 \AA per resolution element and covering the spectral range 7740–8740 \AA . Typically signal-to-noise ratio

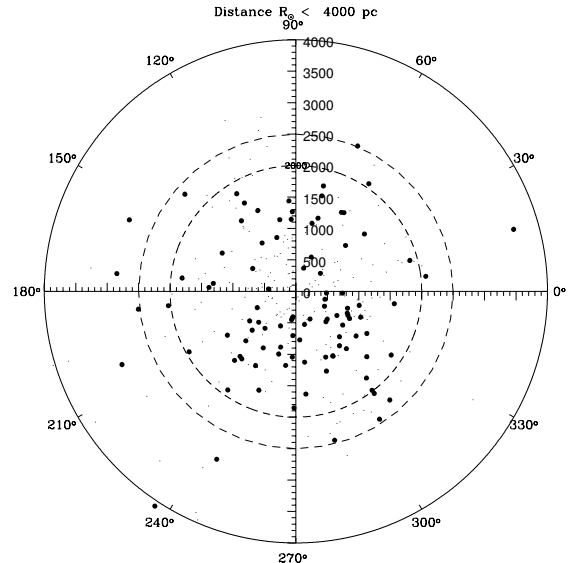


Fig. 1.— Kernel output from 1-D RV space (V_r) for M67. (a) kernel smoothed image of all stars used in the analysis. (b) kernel smoothed image for stars not selected to be with cluster radius (Dias et al. 2002b). (c) Subtraction of (a) $-$ (b) (d) 1-D Gaussian fit to (c). The “cluster” fit distribution is used to determine P_c^V .

(S/N) of typically 10 or better were observed. Approximately 10–100 of the 133 available fibers were used to observe cluster proper motion member candidates; In fields with less than 50 proper motion member candidates, additional stars in the fields of view were targeted selected from the UNSO A2.0 catalog to search for additional clusters members at fainter magnitudes than the ~ 13.5 magnitude limit of the TYCHO2 survey. Any remaining fibers were used for sky observations. To aid the RV calibration, multiple (6 to 13) RV standards were observed each run, where each “observation” of an RV standard entails sending the light down 7–12 different fibers, yielding many dozen individual spectra of RV standards.

WIYN Data

Spectroscopic data were obtained using the Hydra multiobject spectrograph on the 3.5-m WIYN telescope at Kitt Peak National Observatory (KPNO). Table 1 lists the clusters observed and some of their basic properties (Run 5). Data were taken using the Hydra multiobject spectrograph and a 2048×2048 pixel CCD (Red Bench Camera) on the nights of 2003 September 14–18. The data were taken using the echelle ($316@63.4$) grating in 6th order, yielding a dispersion of 0.66 \AA per resolution element and covering the spectral range 8220–8800 \AA . Typically signal-to-noise ratio (S/N) of typically 10 or better were observed. Approximately 10–100 of the 133 available fibers were used to observe cluster proper motion

member candidates; In fields with less than 40 proper motion member candidates, additional stars in the fields of view were targeted selected from the UNSO A2.0 catalogue to search for additional clusters members, with remaining fibers used for sky observations. For RV calibration, multiple RV standards were observed, where each “observation” of an RV standard entails sending the light down 2–5 different fibers.

Basic Reduction

After basic processing the data were run through the *IRAF* routine *dohydra* to a wavelength calibrated 1-D spectrum. The script is used to perform a number of tasks. First, the spectra are transformed from a 2-D image to a 1-D spectrum by fitting a polynomial to trace of the spectrum. The spectra are extracted and calibrated to a comparison lamp spectrum. Exposures of a hollow cathode lamp combined with He, Ne, Ar, and Xe lamps taken at each pointing provide a comparison spectrum yielding at least 11 emission lines roughly evenly distributed over the wavelength range of 8000–8680 Å, which is the range used for RV measurements in §4.2. This comparison spectrum is then used to provide a wavelength solution for each object spectrum. The spectrum is then dispersion corrected, which results in a resampling of the data and sky subtracts the data and standard star spectra interactively by using the *IRAF* all of the extracted spectra have the same end points and number of resulting pixels so that all of the spectra are sampled the same for input for the radial velocity determination program described below.

Radial Velocity Determination

Several strategies are employed to improve upon standard radial velocity techniques and achieve a velocity precision better than 1/20 of a resolution element. The reduction to radial velocities employed essentially the classical cross-correlation methodology of Tonry & Davis (1979). Reliable kinematical information is contained only in the slopes of unblended absorption features that are known to be present in the range of spectral types observed. Therefore, the template input to the correlator is prepared from a high signal-to-noise (S/N) master from which the continuum is eliminated with a zero phase-shift, high pass filter shaped to minimize sideband “ringing”. After filtering, the resulting spectrum is multiplied by a mask that is zero everywhere except at a set of rest frame wavelengths of low ionization or low excitation transitions of elements observed in moderately metal deficient stars; these lines are taken from stellar atmospheric abundance studies of the anticipated candidate spectral types, with each feature passed through a Gaussian profile of unit amplitude and roughly 1.2 times the spectrometer instrumental profile (about

0.75 Å). This mask is wavelength-shifted to match the Doppler velocity of the master; a visual check for sideband symmetry assures that no residual bias remains. The low frequency portion of the spectrum is discarded, leaving a working template with a mean of zero. The target data stream is similarly high-pass filtered. This approach provides an additional major advantage to our kinematic endeavor. Since the output of the correlator is affected only by the strength of the selected spectral feature compared to that in the master, the line list used may be tailored to respond well to a fairly broad range of stellar temperature, gravity, and abundance levels. With spurious or unknown features eliminated by the list selection, we can abandon the requirement that a template match as closely as possible the spectrum of the unknown candidate.

Radial Velocity Error Analysis

All radial velocities were derived using *IRAF*’s *FXCOR* package, which was first used to determine RVs for the standard stars. The RVs of standard stars were measured by cross-correlating each standard star spectrum against every other Fourier-filtered standard star spectrum. The resulting RVs for each individual spectra were averaged and the standard deviation measured; the results are presented in Table 5. Average velocity uncertainties for the individual Hydra standard spectrum are $\sigma_v \sim 1 \text{ km s}^{-1}$ for standard star spectra with $S/N \geq 30$. Further information about the data reduction and RV analysis are described in detail in Frinchaboy & Majewski (2006).

We determined our RV errors from a prescription described in Vogt et al. (1995), which is based on the analysis of repeated standard stars spectrum taken through multiple fibers. The Tonry–Davis Ratio (Tonry & Davis 1979, TDR) for each spectrum, measured from *FXCOR*, scales approximately with S/N , which allows us to determine the radial velocity error using the following equation:

$$\text{Error } V_r = \frac{\alpha}{(1 + \text{TDR})} \quad (1)$$

where α is a constant calibrated by the standard star data, as described in Frinchaboy & Majewski (2006).

The heliocentric RV (V_r) measurements for cluster target stars with a TDR greater than 5 ($S/N \geq 3$), yield RVs with errors of 0.5–5 km s^{-1} .

Membership Determination and Measurement of Cluster Bulk Kinematical Parameters

One of the most complicated problems with working on open clusters is the contamination problems associated with being found within the Galactic plane. To determine the bulk motion of clusters one must first isolate cluster members for the dominant field population. To accomplish this we have modified a technique to do just

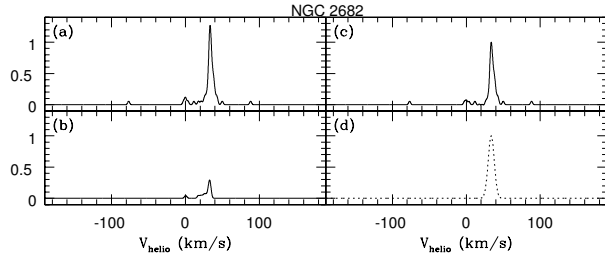


Fig. 2.— Kernel output from 1-D RV space (V_r) for M67. (a) Kernel smoothed image of all stars used in the analysis. (b) Kernel smoothed image for stars not selected to be with cluster radius (Dias et al. 2002b). (c) Subtraction of (a)–(b). (d) 1-D Gaussian fit to (c). The “cluster” fit distribution is used to determine P_c^V .

that. The star’s proper motion, RV and spacial distribution are used as inputs for a kernel based technique described below, which allows the cluster bulk motion to be determined from stars with high membership probabilities.

Non-Parametric Frequency Function

The membership probability of star was determined by fitted a Gaussian distribution function to the data. The best fit Gaussian in RV, had a full width half max (FWHM) of 3 km s^{-1} , as open clusters are known to have intrinsic velocity dispersions of less than 1 km s^{-1} the width of the distribution was fitted to the worst cases of the measured errors in the analyzed stars. We have chosen to use a empirical non-parametric technique to determine cluster membership. The technique is modified from that described in Galadí-Enríquez et al. (1998), which incorporates a kernel estimator technique (Hand 1982) to measure the phase space distribution. The two dimensional kernel function $K(a, b)$ (or 1-D $K(c)$) is used to Gaussian smooth the data over the parameter space following the Galadí-Enríquez et al. (1998) formulation. The phase-space smoothing is accomplished by using the normalized kernel function in 2-D:

$$\int_{-\infty}^{\infty} \int_{-\infty}^{\infty} K(a, b) da db = 1, \quad (2)$$

This technique is fully described in Frinchaboy & Majewski (2006).

The bulk motion of the cluster was measured in the three dimensions. Member stars were used to measure an error weighted mean values for each of the RV and μ measures of the clusters. The method used is shown below to produce the RV error weighted mean and the resulting net error in this determination. The cluster bulk RV is calculated using cluster members using:

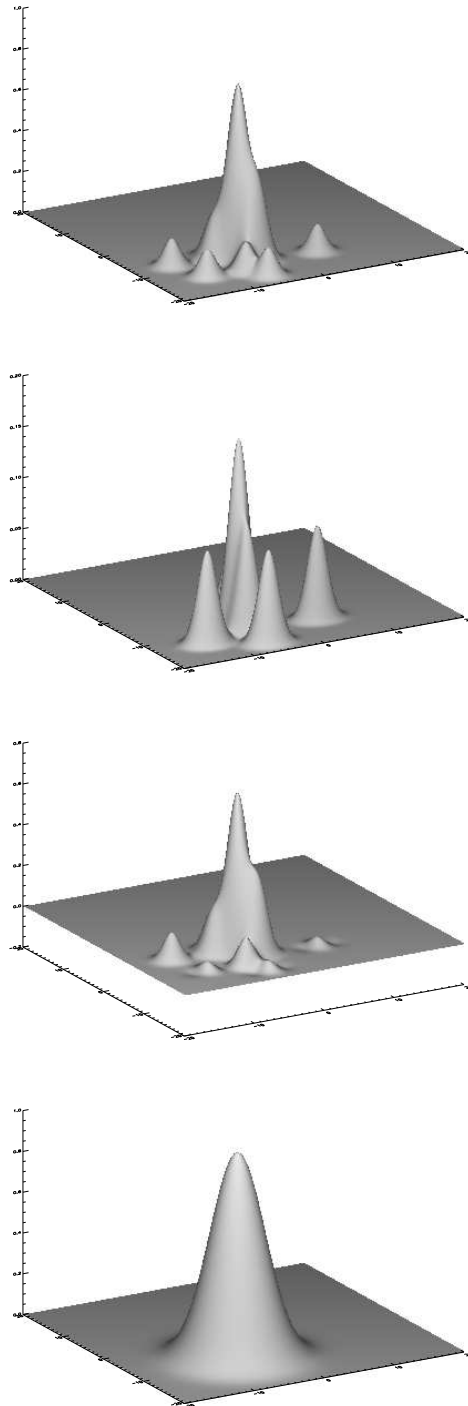


Fig. 3.— Kernel output from 2-D μ space ($\mu_{\alpha \cos(\delta)}, \mu_{\delta}$) for M67. (a) kernel smoothed image of all stars used in the analysis. (b) kernel smoothed image for stars not selected to be RV members (see Figure 1; $P_c^V < 0.5$). (c) Subtraction of (a)–(b). (d) 2-D Gaussian fit to (c). The “cluster” fit distribution is used to determine P_c^K .

$$V_r = \frac{\sum_{i=1}^n \left(\frac{V_{i,r}}{\sigma_{i,V_r}^2} \right)}{\sum_{i=1}^n \left(\frac{1}{\sigma_{i,V_r}^2} \right)} \quad (3)$$

and the errors by,

$$\sigma_{V_r} = \frac{1}{\sqrt{\sum_{i=1}^n \left(\frac{1}{\sigma_{i,V_r}^2} \right)}}. \quad (4)$$

The cluster bulk μ are calculated as above using the following equation.

$$\mu_{\alpha \cos(\delta)} = \frac{\sum_{i=1}^n \left(\frac{\mu_{i,\alpha \cos(\delta)}}{\sigma_{i,\mu_{\alpha \cos(\delta)}}^2} \right)}{\sum_{i=1}^n \left(\frac{1}{\sigma_{i,\mu_{\alpha \cos(\delta)}}^2} \right)} \quad (5)$$

The resulting kernel output for NGC 2682 (M67) is presented in Figures 1 & 2. The full resulting cluster bulk motions are used to investigate the rotation curve of the Galaxy. Full data for this 83 cluster sample is beyond the scope and page limit of this paper and will be presented in a future *Astrophysical Journal Supplement* series contribution (Frinchaboy, *in preparation*).

The Galactic Rotation Curve

For this preliminary analysis of the data, we have fit the data to determine the local Galactic rotation curve ($\Theta(R)$). We have used two different methods to determine $\Theta(R)$ from the present data, one using only RVs for 55 clusters outside of $\pm 30^\circ$ from $l = 0^\circ$ and 180° and an assumption of circular orbits (Brand & Blitz 1993, Eq. 6), and the other using the full space motions of the clusters (Frink et al. 1996, Eq. 7).

$$\Theta_{RV} = R \left(\frac{V_{lsr}}{R_0 \sin l \cos b} \right) + \Omega_0 R \quad (6)$$

$$\begin{aligned} \Theta_{3D} = & \Omega_0 R + (U - \Omega_0 Y) \sin(\tan^{-1}(X/Y)) \\ & + (V - \Omega_0 X) \cos(\tan^{-1}(X/Y)) \end{aligned} \quad (7)$$

where $\Omega_0 = \Theta_0/R_0$ and X and Y are the Galactic Cartesian coordinates in the left-handed system, and U and V are the projected velocities along the X and Y directions.

Both methods require an assumed Θ_0 and R_0 , which we vary. The results of the two methods were then compared to determine at what Θ_0 and R_0 the $\Theta(R)$ trends are consistent. This comparison on the parameter space is shown in Fig. 5. We fit the resulting rotation curves

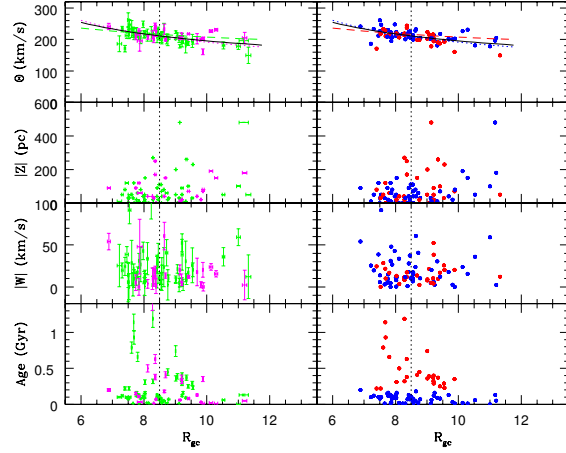


Fig. 4.— (a) (b) (c) (d) (e) (f) (g) (h) (i) (j) (k) (l) (m) (n) (o) (p) (q) (r) (s) (t) (u) (v) (w) (x) (y) (z) (aa) (ab) (ac) (ad) (ae) (af) (ag) (ah) (ai) (aj) (ak) (al) (am) (an) (ao) (ap) (aq) (ar) (as) (at) (au) (av) (aw) (ax) (ay) (az) (ba) (bb) (bc) (bd) (be) (bf) (bg) (bh) (bi) (bj) (bk) (bl) (bm) (bn) (bo) (bp) (bq) (br) (bs) (bt) (bu) (bv) (bw) (bx) (by) (bz) (ca) (cb) (cc) (cd) (ce) (cf) (cg) (ch) (ci) (cj) (ck) (cl) (cm) (cn) (co) (cp) (cq) (cr) (cs) (ct) (cu) (cv) (cw) (cx) (cy) (cz) (da) (db) (dc) (dd) (de) (df) (dg) (dh) (di) (dj) (dk) (dl) (dm) (dn) (do) (dp) (dq) (dr) (ds) (dt) (du) (dv) (dw) (dx) (dy) (dz) (ea) (eb) (ec) (ed) (ee) (ef) (eg) (eh) (ei) (ej) (ek) (el) (em) (en) (eo) (ep) (eq) (er) (es) (et) (eu) (ev) (ew) (ex) (ey) (ez) (fa) (fb) (fc) (fd) (fe) (ff) (fg) (fh) (fi) (fj) (fk) (fl) (fm) (fn) (fo) (fp) (fq) (fr) (fs) (ft) (fu) (fv) (fw) (fx) (fy) (fz) (ga) (gb) (gc) (gd) (ge) (gf) (gg) (gh) (gi) (gj) (gk) (gl) (gm) (gn) (go) (gp) (gq) (gr) (gs) (gt) (gu) (gv) (gw) (gx) (gy) (gz) (ha) (hb) (hc) (hd) (he) (hf) (hg) (hh) (hi) (hj) (hk) (hl) (hm) (hn) (ho) (hp) (hq) (hr) (hs) (ht) (hu) (hv) (hw) (hx) (hy) (hz) (ia) (ib) (ic) (id) (ie) (if) (ig) (ih) (ii) (ij) (ik) (il) (im) (in) (io) (ip) (iq) (ir) (is) (it) (iu) (iv) (iw) (ix) (iy) (iz) (ja) (jb) (jc) (jd) (je) (jf) (jg) (jh) (ji) (jj) (jk) (jl) (jm) (jn) (jo) (jp) (jq) (jr) (js) (jt) (ju) (jv) (jw) (jx) (jy) (jz) (ka) (kb) (kc) (kd) (ke) (kf) (kg) (kh) (ki) (kj) (kk) (kl) (km) (kn) (ko) (kp) (kq) (kr) (ks) (kt) (ku) (kv) (kw) (kx) (ky) (kz) (la) (lb) (lc) (ld) (le) (lf) (lg) (lh) (li) (lj) (lk) (ll) (lm) (ln) (lo) (lp) (lq) (lr) (ls) (lt) (lu) (lv) (lw) (lx) (ly) (lz) (ma) (mb) (mc) (md) (me) (mf) (mg) (mh) (mi) (mj) (mk) (ml) (mm) (mn) (mo) (mp) (mq) (mr) (ms) (mt) (mu) (mv) (mw) (mx) (my) (mz) (na) (nb) (nc) (nd) (ne) (nf) (ng) (nh) (ni) (nj) (nk) (nl) (nm) (nn) (no) (np) (nq) (nr) (ns) (nt) (nu) (nv) (nw) (nx) (ny) (nz) (oa) (ob) (oc) (od) (oe) (of) (og) (oh) (oi) (oj) (ok) (ol) (om) (on) (oo) (op) (oq) (or) (os) (ot) (ou) (ov) (ow) (ox) (oy) (oz) (pa) (pb) (pc) (pd) (pe) (pf) (pg) (ph) (pi) (pj) (pk) (pl) (pm) (pn) (po) (pp) (pq) (pr) (ps) (pt) (pu) (pv) (pw) (px) (py) (pz) (qa) (qb) (qc) (qd) (qe) (qf) (qg) (qh) (qi) (qj) (qk) (ql) (qm) (qn) (qo) (qp) (qq) (qr) (qs) (qt) (qu) (qv) (qw) (qx) (qy) (qz) (ra) (rb) (rc) (rd) (re) (rf) (rg) (rh) (ri) (rj) (rk) (rl) (rm) (rn) (ro) (rp) (rq) (rr) (rs) (rt) (ru) (rv) (rw) (rx) (ry) (rz) (sa) (sb) (sc) (sd) (se) (sf) (sg) (sh) (si) (sj) (sk) (sl) (sm) (sn) (so) (sp) (sq) (sr) (ss) (st) (su) (sv) (sw) (sx) (sy) (sz) (ta) (tb) (tc) (td) (te) (tf) (tg) (th) (ti) (tj) (tk) (tl) (tm) (tn) (to) (tp) (tq) (tr) (ts) (tt) (tu) (tv) (tw) (tx) (ty) (tz) (ua) (ub) (uc) (ud) (ue) (uf) (ug) (uh) (ui) (uj) (uk) (ul) (um) (un) (uo) (up) (uq) (ur) (us) (ut) (uu) (uv) (uw) (ux) (uy) (uz) (va) (vb) (vc) (vd) (ve) (vf) (vg) (vh) (vi) (vj) (vk) (vl) (vm) (vn) (vo) (vp) (vq) (vr) (vs) (vt) (vu) (vv) (vw) (vx) (vy) (vz) (wa) (wb) (wc) (wd) (we) (wf) (wg) (wh) (wi) (wj) (wk) (wl) (wm) (wn) (wo) (wp) (wq) (wr) (ws) (wt) (wu) (wv) (ww) (wx) (wy) (wz) (xa) (xb) (xc) (xd) (xe) (xf) (xg) (xh) (xi) (xj) (xk) (xl) (xm) (xn) (xo) (xp) (xq) (xr) (xs) (xt) (xu) (xv) (xw) (xx) (xy) (xz) (ya) (yb) (yc) (yd) (ye) (yf) (yg) (yh) (yi) (yj) (yk) (yl) (ym) (yn) (yo) (yp) (yq) (yr) (ys) (yt) (yu) (yv) (yw) (yx) (yy) (yz) (za) (zb) (zc) (zd) (ze) (zf) (zg) (zh) (zi) (zj) (zk) (zl) (zm) (zn) (zo) (zp) (zq) (zr) (zs) (zt) (zu) (zv) (zw) (zx) (zy) (zz) (Aa) (Ab) (Ac) (Ad) (Ae) (Af) (Ag) (Ah) (Ai) (Aj) (Ak) (Al) (Am) (An) (Ao) (Ap) (Aq) (Ar) (As) (At) (Au) (Av) (Aw) (Ax) (Ay) (Az) (Ba) (Bb) (Bc) (Bd) (Be) (Bf) (Bg) (Bh) (Bi) (Bj) (Bk) (Bl) (Bm) (Bn) (Bo) (Bp) (Bq) (Br) (Bs) (Bt) (Bu) (Bv) (Bw) (Bx) (By) (Bz) (Ca) (Cb) (Cc) (Cd) (Ce) (Cf) (Cg) (Ch) (Ci) (Cj) (Ck) (Cl) (Cm) (Cn) (Co) (Cp) (Cq) (Cr) (Cs) (Ct) (Cu) (Cv) (Cw) (Cx) (Cy) (Cz) (Da) (Db) (Dc) (Dd) (De) (Df) (Dg) (Dh) (Di) (Dj) (Dk) (Dl) (Dm) (Dn) (Do) (Dp) (Dq) (Dr) (Ds) (Dt) (Du) (Dv) (Dw) (Dx) (Dy) (Dz) (Ea) (Eb) (Ec) (Ed) (Ee) (Ef) (Eg) (Eh) (Ei) (Ej) (Ek) (El) (Em) (En) (Eo) (Ep) (Eq) (Er) (Es) (Et) (Eu) (Ev) (Ew) (Ex) (Ey) (Ez) (Fa) (Fb) (Fc) (Fd) (Fe) (Ff) (Fg) (Fh) (Fi) (Fj) (Fk) (Fl) (Fm) (Fn) (Fo) (Fp) (Fq) (Fr) (Fs) (Ft) (Fu) (Fv) (Fw) (Fx) (Fy) (Fz) (Ga) (Gb) (Gc) (Gd) (Ge) (Gf) (Gg) (Gh) (Gi) (Gj) (Gk) (Gl) (Gm) (Gn) (Go) (Gp) (Gq) (Gr) (Gs) (Gt) (Gu) (Gv) (Gw) (Gx) (Gy) (Gz) (Ha) (Hb) (Hc) (Hd) (He) (Hf) (Hg) (Hh) (Hi) (Hj) (Hk) (Hl) (Hm) (Hn) (Ho) (Hp) (Hq) (Hr) (Hs) (Ht) (Hu) (Hv) (Hw) (Hx) (Hy) (Hz) (Ia) (Ib) (Ic) (Id) (Ie) (If) (Ig) (Ih) (Ii) (Ij) (Ik) (Il) (Im) (In) (Io) (Ip) (Iq) (Ir) (Is) (It) (Iu) (Iv) (Iw) (Ix) (Iy) (Iz) (Ja) (Jb) (Jc) (Jd) (Je) (Jf) (Jg) (Jh) (Ji) (Jj) (Jk) (Jl) (Jm) (Jn) (Jo) (Jp) (Jq) (Jr) (Js) (Jt) (Ju) (Jv) (Jw) (Jx) (Jy) (Jz) (Ka) (Kb) (Kc) (Kd) (Ke) (Kf) (Kg) (Kh) (Ki) (Kj) (Kk) (Kl) (Km) (Kn) (Ko) (Kp) (Kq) (Kr) (Ks) (Kt) (Ku) (Kv) (Kw) (Kx) (Ky) (Kz) (La) (Lb) (Lc) (Ld) (Le) (Lf) (Lg) (Lh) (Li) (Lj) (Lk) (Ll) (Lm) (Ln) (Lo) (Lp) (Lq) (Lr) (Ls) (Lt) (Lu) (Lv) (Lw) (Lx) (Ly) (Lz) (Ma) (Mb) (Mc) (Md) (Me) (Mf) (Mg) (Mh) (Mi) (Mj) (Mk) (Ml) (Mm) (Mn) (Mo) (Mp) (Mq) (Mr) (Ms) (Mt) (Mu) (Mv) (Mw) (Mx) (My) (Mz) (Na) (Nb) (Nc) (Nd) (Ne) (Nf) (Ng) (Nh) (Ni) (Nj) (Nk) (Nl) (Nm) (Nn) (No) (Np) (Nq) (Nr) (Ns) (Nt) (Nu) (Nv) (Nw) (Nx) (Ny) (Nz) (Oa) (Ob) (Oc) (Od) (Oe) (Of) (Og) (Oh) (Oi) (Oj) (Ok) (Ol) (Om) (On) (Oo) (Op) (Oq) (Or) (Os) (Ot) (Ou) (Ov) (Ow) (Ox) (Oy) (Oz) (Pa) (Pb) (Pc) (Pd) (Pe) (Pf) (Pg) (Ph) (Pi) (Pj) (Pk) (Pl) (Pm) (Pn) (Po) (Pp) (Pq) (Pr) (Ps) (Pt) (Pu) (Pv) (Pw) (Px) (Py) (Pz) (Qa) (Qb) (Qc) (Qd) (Qe) (Qf) (Qg) (Qh) (Qi) (Qj) (Qk) (Ql) (Qm) (Qn) (Qo) (Qp) (Qq) (Qr) (Qs) (Qt) (Qu) (Qv) (Qw) (Qx) (Qy) (Qz) (Ra) (Rb) (Rc) (Rd) (Re) (Rf) (Rg) (Rh) (Ri) (Rj) (Rk) (Rl) (Rm) (Rn) (Ro) (Rp) (Rq) (Rr) (Rs) (Rt) (Ru) (Rv) (Rw) (Rx) (Ry) (Rz) (Sa) (Sb) (Sc) (Sd) (Se) (Sf) (Sg) (Sh) (Si) (Sj) (Sk) (Sl) (Sm) (Sn) (So) (Sp) (Sq) (Sr) (Ss) (St) (Su) (Sv) (Sw) (Sx) (Sy) (Sz) (Ta) (Tb) (Tc) (Td) (Te) (Tf) (Tg) (Th) (Ti) (Tj) (Tk) (Tl) (Tm) (Tn) (To) (Tp) (Tq) (Tr) (Ts) (Tt) (Tu) (Tv) (Tw) (Tx) (Ty) (Tz) (Ua) (Ub) (Uc) (Ud) (Ue) (Uf) (Ug) (Uh) (Ui) (Uj) (Uk) (Ul) (Um) (Un) (Uo) (Up) (Uq) (Ur) (Us) (Ut) (Uu) (Uv) (Uw) (Ux) (Uy) (Uz) (Va) (Vb) (Vc) (Vd) (Ve) (Vf) (Vg) (Vh) (Vi) (Vj) (Vk) (Vl) (Vm) (Vn) (Vo) (Vp) (Vq) (Vr) (Vs) (Vt) (Vu) (Vv) (Vw) (Vx) (Vy) (Vz) (Wa) (Wb) (Wc) (Wd) (We) (Wf) (Wg) (Wh) (Wi) (Wj) (Wk) (Wl) (Wm) (Wn) (Wo) (Wp) (Wq) (Wr) (Ws) (Wt) (Wu) (Wv) (Ww) (Wx) (Wy) (Wz) (Xa) (Xb) (Xc) (Xd) (Xe) (Xf) (Xg) (Xh) (Xi) (Xj) (Xk) (Xl) (Xm) (Xn) (Xo) (Xp) (Xq) (Xr) (Xs) (Xt) (Xu) (Xv) (Xw) (Xx) (Xy) (Xz) (Ya) (Yb) (Yc) (Yd) (Ye) (Yf) (Yg) (Yh) (Yi) (Yj) (Yk) (Yl) (Ym) (Yn) (Yo) (Yp) (Yq) (Yr) (Ys) (Yt) (Yu) (Yv) (Yw) (Yx) (Yy) (Yz) (Za) (Zb) (Zc) (Zd) (Ze) (Zf) (Zg) (Zh) (Zi) (Zj) (Zk) (Zl) (Zm) (Zn) (Zo) (Zp) (Zq) (Zr) (Zs) (Zt) (Zu) (Zv) (Zw) (Zx) (Zy) (Zz) (aa) (ab) (ac) (ad) (ae) (af) (ag) (ah) (ai) (aj) (ak) (al) (am) (an) (ao) (ap) (aq) (ar) (as) (at) (au) (av) (aw) (ax) (ay) (az) (ba) (bb) (bc) (bd) (be) (bf) (bg) (bh) (bi) (bj) (bk) (bl) (bm) (bn) (bo) (bp) (bq) (br) (bs) (bt) (bu) (bv) (bw) (bx) (by) (bz) (ca) (cb) (cc) (cd) (ce) (cf) (cg) (ch) (ci) (cj) (ck) (cl) (cm) (cn) (co) (cp) (cq) (cr) (cs) (ct) (cu) (cv) (cw) (cx) (cy) (cz) (da) (db) (dc) (dd) (de) (df) (dg) (dh) (di) (dj) (dk) (dl) (dm) (dn) (do) (dp) (dq) (dr) (ds) (dt) (du) (dv) (dw) (dx) (dy) (dz) (ea) (eb) (ec) (ed) (ee) (ef) (eg) (eh) (ei) (ej) (ek) (el) (em) (en) (eo) (ep) (eq) (er) (es) (et) (eu) (ev) (ew) (ex) (ey) (ez) (fa) (fb) (fc) (fd) (fe) (ff) (fg) (fh) (fi) (fj) (fk) (fl) (fm) (fn) (fo) (fp) (fq) (fr) (fs) (ft) (fu) (fv) (fw) (fx) (fy) (fz) (ga) (gb) (gc) (gd) (ge) (gf) (gg) (gh) (gi) (gj) (gk) (gl) (gm) (gn) (go) (gp) (gq) (gr) (gs) (gt) (gu) (gv) (gw) (gx) (gy) (gz) (ha) (hb) (hc) (hd) (he) (hf) (hg) (hh) (hi) (hj) (hk) (hl) (hm) (hn) (ho) (hp) (hq) (hr) (hs) (ht) (hu) (hv) (hw) (hx) (hy) (hz) (ia) (ib) (ic) (id) (ie) (if) (ig) (ih) (ii) (ij) (ik) (il) (im) (in) (io) (ip) (iq) (ir) (is) (it) (iu) (iv) (iw) (ix) (iy) (iz) (ja) (jb) (jc) (jd) (je) (jf) (jg) (jh) (ji) (jj) (jk) (jl) (jm) (jn) (jo) (jp) (jq) (jr) (js) (jt) (ju) (jv) (jw) (jx) (jy) (jz) (ka) (kb) (kc) (kd) (ke) (kf) (kg) (kh) (ki) (kj) (kk) (kl) (km) (kn) (ko) (kp) (kq) (kr) (ks) (kt) (ku) (kv) (kw) (kx) (ky) (kz) (la) (lb) (lc) (ld) (le) (lf) (lg) (lh) (li) (lj) (lk) (ll) (lm) (ln) (lo) (lp) (lq) (lr) (ls) (lt) (lu) (lv) (lw) (lx) (ly) (lz) (ma) (mb) (mc) (md) (me) (mf) (mg) (mh) (mi) (mj) (mk) (ml) (mm) (mn) (mo) (mp) (mq) (mr) (ms) (mt) (mu) (mv) (mw) (mx) (my) (mz) (na) (nb) (nc) (nd) (ne) (nf) (ng) (nh) (ni) (nj) (nk) (nl) (nm) (nn) (no) (np) (nq) (nr) (ns) (nt) (nu) (nv) (nw) (nx) (ny) (nz) (oa) (ob) (oc) (od) (oe) (of) (og) (oh) (oi) (oj) (ok) (ol) (om) (on) (oo) (op) (oq) (or) (os) (ot) (ou) (ov) (ow) (ox) (oy) (oz) (pa) (pb) (pc) (pd) (pe) (pf) (pg) (ph) (pi) (pj) (pk) (pl) (pm) (pn) (po) (pp) (pq) (pr) (ps) (pt) (pu) (pv) (pw) (px) (py) (pz) (qa) (qb) (qc) (qd) (qe) (qf) (qg) (qh) (qi) (qj) (qk) (ql) (qm) (qn) (qo) (qp) (qq) (qr) (qs) (qt) (qu) (qv) (qw) (qx) (qy) (qz) (ra) (rb) (rc) (rd) (re) (rf) (rg) (rh) (ri) (rj) (rk) (rl) (rm) (rn) (ro) (rp) (rq) (rr) (rs) (rt) (ru) (rv) (rw) (rx) (ry) (rz) (sa) (sb) (sc) (sd) (se) (sf) (sg) (sh) (si) (sj) (sk) (sl) (sm) (sn) (so) (sp) (sq) (sr) (ss) (st) (su) (sv) (sw) (sx) (sy) (sz) (ta) (tb) (tc) (td) (te) (tf) (tg) (th) (ti) (tj) (tk) (tl) (tm) (tn) (to) (tp) (tq) (tr) (ts) (tt) (tu) (tv) (tw) (tx) (ty) (tz) (ua) (ub) (uc) (ud) (ue) (uf) (ug) (uh) (ui) (uj) (uk) (ul) (um) (un) (uo) (up) (uq) (ur) (us) (ut) (uu) (uv) (uw) (ux) (uy) (uz) (va) (vb) (vc) (vd) (ve) (vf) (vg) (vh) (vi) (vj) (vk) (vl) (vm) (vn) (vo) (vp) (vq) (vr) (vs) (vt) (vu) (vv) (vw) (vx) (vy) (vz) (wa) (wb) (wc) (wd) (we) (wf) (wg) (wh) (wi) (wj) (wk) (wl) (wm) (wn) (wo) (wp) (wq) (wr) (ws) (wt) (wu) (wv) (ww) (wx) (wy) (wz) (xa) (xb) (xc) (xd) (xe) (xf) (xg) (xh) (xi) (xj) (xk) (xl) (xm) (xn) (xo) (xp) (xq) (xr) (xs) (xt) (xu) (xv) (xw) (xx) (xy) (xz) (ya) (yb) (yc) (yd) (ye) (yf) (yg) (yh) (yi) (yj) (yk) (yl) (ym) (yn) (yo) (yp) (yq) (yr) (ys) (yt) (yu) (yv) (yw) (yx) (yy) (yz) (za) (zb) (zc) (zd) (ze) (zf) (zg) (zh) (zi) (zj) (zk) (zl) (zm) (zn) (zo) (zp) (zq) (zr) (zs) (zt) (zu) (zv) (zw) (zx) (zy) (zz) (Aa) (Ab) (Ac) (Ad) (Ae) (Af) (Ag) (Ah) (Ai) (Aj) (Ak) (Al) (Am) (An) (Ao) (Ap) (Aq) (Ar) (As) (At) (Au) (Av) (Aw) (Ax) (Ay) (Az) (Ba) (Bb) (Bc) (Bd) (Be) (Bf) (Bg) (Bh) (Bi) (Bj) (Bk) (Bl) (Bm) (Bn) (Bo) (Bp) (Bq) (Br) (Bs) (Bt) (Bu) (Bv) (Bw) (Bx) (By) (Bz) (Ca) (Cb) (Cc) (Cd) (Ce) (Cf) (Cg) (Ch) (Ci) (Cj) (Ck) (Cl) (Cm) (Cn) (Co) (Cp) (Cq) (Cr) (Cs) (Ct) (Cu) (Cv) (Cw) (Cx) (Cy) (Cz) (Da) (Db) (Dc) (Dd) (De) (Df) (Dg) (Dh) (Di) (Dj) (Dk) (Dl) (Dm) (Dn) (Do) (Dp) (Dq) (Dr) (Ds) (Dt) (Du) (Dv) (Dw) (Dx) (Dy) (Dz) (Ea) (Eb) (Ec) (Ed) (Ee) (Ef) (Eg) (Eh) (Ei) (Ej) (Ek) (El) (Em) (En) (Eo) (Ep) (Eq) (Er) (Es) (Et) (Eu) (Ev) (Ew) (Ex) (Ey) (Ez) (Fa) (Fb) (Fc) (Fd) (Fe) (Ff) (Fg) (Fh) (Fi) (Fj) (Fk) (Fl) (Fm) (Fn) (Fo) (Fp) (Fq) (Fr) (Fs) (Ft) (Fu) (Fv) (Fw) (Fx) (Fy) (Fz) (Ga) (Gb) (Gc) (Gd) (Ge) (Gf) (Gg) (Gh) (Gi) (Gj) (Gk) (Gl) (Gm) (Gn) (Go) (Gp) (Gq) (Gr) (Gs) (Gt) (Gu) (Gv) (Gw) (Gx) (Gy) (Gz) (Ha) (Hb) (Hc) (Hd) (He) (Hf) (Hg) (Hh) (Hi) (Hj) (Hk) (Hl) (Hm) (Hn) (Ho) (Hp) (Hq) (Hr) (Hs) (Ht) (Hu) (Hv) (Hw) (Hx) (Hy) (Hz) (Ia) (Ib) (Ic) (Id) (Ie) (If) (Ig) (Ih) (Ii) (Ij) (Ik) (Il) (Im) (In) (Io) (Ip) (Iq) (Ir) (Is) (It) (Iu) (Iv) (Iw) (Ix) (Iy) (Iz) (Ja) (Jb) (Jc) (Jd) (Je) (Jf) (Jg) (Jh) (Ji) (Jj) (Jk) (Jl) (Jm) (Jn) (Jo) (Jp) (Jq) (Jr) (Js) (Jt) (Ju) (Jv) (Jw) (Jx) (Jy) (Jz) (Ka) (Kb) (Kc) (Kd) (Ke) (Kf) (Kg) (Kh) (Ki) (Kj) (Kk) (Kl) (Km) (Kn) (Ko) (Kp) (Kq) (Kr) (Ks) (Kt) (Ku) (Kv) (Kw) (Kx) (Ky) (Kz) (La) (Lb) (Lc) (Ld) (Le) (Lf) (Lg) (Lh) (Li) (Lj) (Lk) (Ll) (Lm) (Ln) (Lo) (Lp) (Lq) (Lr) (Ls) (Lt) (Lu) (Lv) (Lw) (Lx) (Ly) (Lz) (Ma) (Mb) (Mc) (Md) (Me) (Mf) (Mg) (Mh) (Mi) (Mj) (Mk) (Ml) (Mm) (Mn) (Mo) (Mp) (Mq) (Mr) (Ms) (Mt) (Mu) (Mv) (Mw) (Mx) (My) (Mz) (Na) (Nb) (Nc) (Nd) (Ne) (Nf) (Ng) (Nh) (Ni) (Nj) (Nk) (Nl) (Nm) (Nn) (No) (Np) (Nq) (Nr) (Ns) (Nt) (Nu) (Nv) (Nw) (Nx) (Ny) (Nz) (Oa) (Ob) (Oc) (Od) (Oe) (Of) (Og) (Oh) (Oi) (Oj) (Ok) (Ol) (Om) (On) (Oo) (Op) (Oq) (Or) (Os) (Ot) (Ou) (Ov) (Ow) (Ox) (Oy) (Oz) (Pa) (Pb) (Pc) (Pd) (Pe) (Pf) (Pg) (Ph) (Pi) (Pj) (Pk) (Pl) (Pm) (Pn) (Po) (Pp) (Pq) (Pr) (Ps) (Pt) (Pu) (Pv) (Pw) (Px) (Py) (Pz) (Qa) (Qb) (Qc) (Qd) (Qe) (Qf) (Qg) (Qh) (Qi) (Qj) (Qk) (Ql) (Qm) (Qn) (Qo) (Qp) (Qq) (Qr) (Qs) (Qt) (Qu) (Qv) (Qw) (Qx) (Qy) (Qz) (Ra) (Rb) (Rc) (Rd) (Re) (Rf) (Rg) (Rh) (Ri) (Rj) (Rk) (Rl) (Rm) (Rn) (Ro) (Rp) (Rq) (Rr) (Rs) (Rt) (Ru) (Rv) (Rw) (Rx) (Ry) (Rz) (Sa) (Sb) (Sc) (Sd) (Se) (Sf) (Sg) (Sh) (Si) (Sj) (Sk) (Sl) (Sm) (Sn) (So) (Sp) (Sq) (Sr) (Ss) (St) (Su) (Sv) (Sw) (Sx) (Sy) (Sz) (Ta) (Tb) (Tc) (Td) (Te) (Tf) (Tg) (Th) (Ti) (Tj) (Tk) (Tl) (Tm) (Tn) (To) (Tp) (Tq) (Tr) (Ts) (Tt) (Tu) (Tv) (Tw) (Tx) (Ty) (Tz) (Ua) (Ub) (Uc) (Ud) (Ue) (Uf) (Ug) (Uh) (Ui) (Uj) (Uk) (Ul) (Um) (Un) (Uo) (Up) (Uq) (Ur) (Us) (Ut) (Uu) (Uv) (Uw) (Ux) (Uy) (Uz) (Va) (Vb) (Vc) (Vd) (Ve) (Vf) (Vg) (Vh) (Vi) (Vj) (Vk) (Vl) (Vm) (Vn) (Vo) (Vp) (Vq) (Vr) (Vs) (Vt) (Vu) (Vv) (Vw) (Vx) (Vy) (Vz) (Wa) (Wb) (Wc) (Wd) (We) (Wf) (Wg) (Wh) (Wi) (Wj) (Wk) (Wl) (Wm) (Wn) (Wo) (Wp) (Wq) (Wr) (Ws) (Wt) (Wu) (Wv) (Ww) (Wx) (Wy) (Wz) (Xa) (Xb) (Xc) (Xd) (Xe) (Xf) (Xg) (Xh) (Xi) (Xj) (Xk) (Xl) (Xm) (Xn) (Xo) (Xp) (Xq) (Xr) (Xs) (Xt) (Xu) (Xv) (Xw) (Xx) (Xy) (Xz) (Ya) (Yb) (Yc) (Yd) (Ye) (Yf) (Yg) (Yh) (Yi) (Yj) (Yk) (Yl) (Ym) (Yn) (Yo) (Yp) (Yq) (Yr) (Ys) (Yt) (Yu) (Yv) (Yw) (Yx) (Yy) (Yz) (Za) (Zb) (Zc) (Zd) (Ze) (Zf) (Zg) (Zh) (Zi) (Zj) (Zk) (Zl) (Zm) (Zn) (Zo) (Zp) (Zq) (Zr) (Zs) (Zt) (Zu) (Zv) (Zw) (Zx) (Zy) (Zz) (Aa) (Ab) (Ac) (Ad) (Ae) (Af) (Ag) (Ah) (Ai) (Aj) (Ak) (Al) (Am) (An) (Ao) (Ap) (Aq) (Ar) (As) (At) (Au) (Av) (Aw) (Ax) (Ay) (Az) (Ba) (Bb) (Bc) (Bd) (Be) (Bf) (Bg) (Bh) (Bi) (Bj) (Bk) (Bl) (Bm) (Bn) (Bo) (Bp) (Bq) (Br) (Bs) (Bt) (Bu) (Bv) (Bw) (Bx) (By) (Bz) (Ca) (Cb) (Cc) (Cd) (Ce) (Cf) (Cg) (Ch) (Ci) (Cj) (Ck) (Cl) (Cm) (Cn) (Co) (Cp) (Cq) (Cr) (Cs) (Ct) (Cu) (Cv) (Cw) (Cx) (Cy) (Cz) (Da) (Db) (Dc) (Dd) (De) (Df) (Dg) (Dh) (Di) (Dj) (Dk) (Dl) (Dm) (Dn) (Do) (Dp) (Dq) (Dr) (Ds) (Dt) (Du) (Dv) (Dw) (Dx) (Dy) (Dz) (Ea) (Eb) (Ec) (Ed) (Ee) (Ef) (Eg) (Eh) (Ei) (Ej) (Ek) (El) (Em) (En) (Eo) (Ep) (Eq) (Er) (Es) (Et) (Eu) (Ev) (Ew) (Ex) (Ey) (Ez) (Fa) (Fb) (Fc) (Fd) (Fe) (Ff) (Fg) (Fh) (Fi) (Fj) (Fk) (Fl) (Fm) (Fn) (Fo) (Fp) (Fq) (Fr) (Fs) (Ft) (Fu) (Fv) (Fw) (Fx) (Fy) (Fz) (Ga) (Gb) (Gc) (Gd) (Ge) (Gf) (Gg) (Gh) (Gi) (Gj) (Gk) (Gl) (Gm) (Gn) (Go) (Gp) (Gq) (Gr) (Gs) (Gt) (Gu) (Gv) (Gw) (Gx) (Gy) (Gz) (Ha) (Hb) (Hc) (Hd) (He) (Hf) (Hg) (Hh) (Hi) (Hj) (Hk) (Hl) (Hm) (Hn) (Ho) (Hp) (Hq) (Hr) (Hs) (Ht) (Hu) (Hv) (Hw) (Hx) (Hy) (Hz) (Ia) (Ib) (Ic) (Id) (Ie) (If) (Ig) (Ih) (Ii) (Ij) (Ik) (Il) (Im) (In) (Io) (Ip) (Iq) (Ir) (Is) (It) (Iu) (Iv) (Iw) (Ix) (Iy) (Iz) (Ja) (Jb) (Jc) (Jd) (Je) (Jf) (Jg) (Jh) (Ji) (Jj) (Jk) (Jl) (Jm) (Jn) (Jo) (Jp) (Jq) (Jr) (Js) (Jt) (Ju) (Jv) (Jw) (Jx) (Jy) (Jz) (Ka) (Kb) (Kc) (Kd) (Ke) (Kf) (Kg) (Kh) (Ki) (Kj) (Kk) (Kl) (Km) (Kn) (Ko) (Kp) (Kq) (Kr) (Ks) (Kt) (Ku) (Kv) (Kw) (Kx) (Ky) (Kz) (La) (Lb) (Lc) (Ld) (Le) (Lf) (Lg) (Lh) (Li) (Lj) (Lk) (Ll) (Lm) (Ln) (Lo) (Lp) (Lq) (Lr) (Ls) (Lt) (Lu) (Lv) (Lw) (Lx) (Ly) (Lz) (Ma) (Mb) (Mc) (Md) (Me) (Mf) (Mg) (Mh) (Mi) (Mj) (Mk) (Ml) (Mm) (Mn) (Mo) (Mp) (Mq) (Mr) (Ms) (Mt) (Mu) (Mv) (Mw) (Mx) (My) (Mz) (Na) (Nb) (Nc) (Nd) (Ne) (Nf) (Ng) (Nh) (Ni) (Nj) (Nk) (Nl) (Nm) (Nn) (No) (Np) (Nq) (Nr) (Ns) (Nt) (Nu) (Nv) (Nw) (Nx) (Ny) (Nz) (Oa) (Ob) (Oc) (Od) (Oe) (Of) (Og) (Oh) (Oi) (Oj) (Ok) (Ol) (Om) (On) (Oo) (Op) (Oq) (Or) (Os) (Ot) (Ou) (Ov) (Ow) (Ox) (Oy) (Oz) (Pa) (Pb) (Pc) (Pd) (Pe) (Pf) (Pg) (Ph) (Pi) (Pj) (Pk) (Pl) (Pm) (Pn) (Po) (Pp) (Pq) (Pr) (Ps) (Pt) (Pu) (Pv) (Pw) (Px) (Py) (Pz) (Qa) (Qb) (Qc) (Qd) (Qe) (Qf) (Qg) (Qh) (Qi) (Qj) (Qk) (Ql) (Qm) (Qn) (Qo) (Qp) (Qq) (Qr) (Qs) (Qt) (Qu) (Qv) (Qw) (Qx) (Qy) (Qz) (Ra) (Rb) (Rc) (Rd) (Re) (Rf) (Rg) (Rh) (Ri) (Rj) (Rk) (Rl) (Rm) (Rn) (Ro) (Rp) (Rq) (Rr) (Rs) (Rt) (Ru) (Rv) (Rw) (Rx) (Ry) (Rz) (Sa) (Sb) (Sc) (Sd) (Se) (Sf) (Sg) (Sh) (Si) (Sj) (Sk) (Sl) (Sm) (Sn) (So) (Sp) (Sq) (Sr) (Ss) (St) (Su) (Sv) (Sw) (Sx

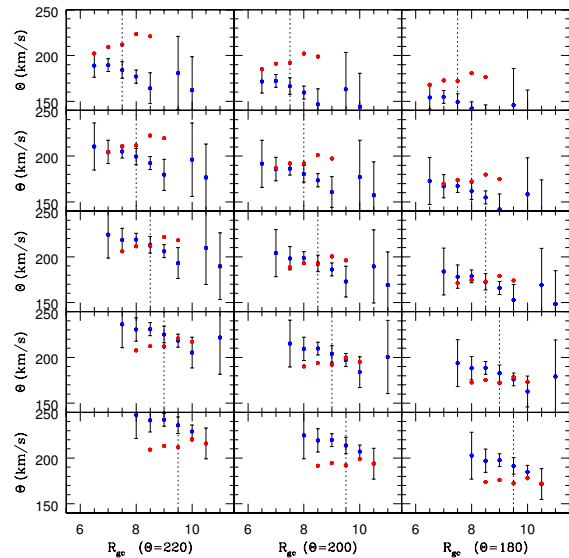


Fig. 5.— Plots of the rotation curve using the RV only method (Θ_{RV} , shown in red) versus the method using the full space motion (Θ_{3D} , shown in blue) for a grid of assumed R_0 and Θ_0 . The parameter space explored here is $R_0 = (7.5, 8.0, 8.5, 9.0, 9.5)$ kpc and $\Theta_0 = (180, 200, 220)$ km s $^{-1}$

Future Work

Future work on this project is to extend the analysis to the complete cluster sample. More than 100 clusters have been observed, listed in Table 2. These clusters will be used to not only measure their orbits, but, once the ensemble is complete, to test the Galactic model used in the orbit integration and thereby the mass and mass distribution of the Galactic disk and the GASS. Additionally, the Galactic velocity field (deviations from circular rotation) and the metallicity distribution with Galactic radius will be explored in completion of my thesis.

Acknowledgments

I would like to thank my primary advisor, Steven Majewski, for his guidance and support of this work. I would also like to thank W. Butler Burton for the useful conversations, Kathryn Johnston for providing the orbit integrator and her expertise, and NOAO for travel support for these thesis project observations. We acknowledge funding by NSF grant AST-0307851, NASA/JPL contract 1228235, the David and Lucile Packard Foundation, a Cottrell Scholar Award from The Research Corporation, and the F.H. Levinson Fund of the Peninsula Community Foundation. The author has also been aided an Aerospace Graduate Research Fellowship, administered by the Virginia Space Grant Consortium, a NASA Graduate Student Researchers Program, and a University

Table 1: Rotation Curve Fitting

Selection	#				Slope	θ_0 (fit)
		a_1	a_2	a_3	(km/s/kpc)	(km/s)
$(R_0, \theta_0) = (8.5, 200)$						
All (3D)	83	0.669	-0.534	0.282	-8.4	190
All (RV)	55	0.490	+0.290	0.485	+3.3	194
Bin (3D)	83	0.488	-0.387	0.477	-4.4	193
Bin (RV)	55	0.539	+0.318	0.434	+4.0	195
$(R_0, \theta_0) = (8.5, 180)$						
All (3D)	83	0.762	-0.524	0.183	-8.5	170
All (RV)	55	0.487	+0.098	0.485	+1.0	175
Bin (3D)	83	0.446	-0.456	0.514	-4.3	173
Bin (RV)	55	0.519	+0.114	0.453	+1.3	175

of Virginia Faculty Senate Dissertation-Year Fellowship.

The Tycho2 catalog is based on observations of the ESA Hipparcos satellite. This research has made use of the USNOFS Image and Catalogue Archive operated by the United States Naval Observatory, Flagstaff Station (<http://www.nofs.navy.mil/data/fchpix/>).

References

- Amaral, L. H., Ortiz, R., Lépine, J. R. D. & Maciel, W. J. 1996, MNRAS, 281, 339
- Brand, J. & Blitz, L. 1993, A&AS, 275, 67
- Dias, W.S., Lépine, J.R.D. & Alessi, B.S. 2001, A&A, 376, 441
- Dias, W.S., Lépine, J.R.D. & Alessi, B.S. 2002a, A&A, 388, 168
- Dias, W.S., Alessi, B.S., Moitinho, Lépine, J.R.D. & Alessi, B.S. 2002b, A&A, 389, 8718
- Fich, M., Blitz, L., & Stark, A.A. 1989, ApJ, 342, 272
- Frinchaboy, P. M. & Majewski, S. R. 2006, AJ, *submitted*
- Frink, S., Fuchs, B., Rser, S., & Wielen, R. 1996, A&A, 314, 430
- Galadí-Enríquez, D., Jordi, C. & Trullols, E. 1998, A&A, 337, 125
- Hand D.J. 1982, Kernel Discriminant Analysis, Chichester Research Studies Press
- Pont, F., Mayor, M., & Burki, G. 1994, A&A, 285, 415
- Tonry, J. & Davis, M. 1979, AJ, 84, 1511
- Vogt, S. S., Mateo, M., Olszewski, E. W. & Keane, M. J. 1995, AJ, 109, 151

Table 2: Cluster Basic Parameters

Cluster	$\alpha_{2000.0}$	$\delta_{2000.0}$	l (°)	b (°)	d(pc)	Log(Age)	Diam(')	Run
NGC 129	00:30:00	+60:13:06	120.2701875	+1.4566728	1625	7.886	19	5
NGC 381	01:08:19	+61:35:00	294.3672154	+0.1870996	1148	8.505	6	5
NGC 457	01:19:35	+58:17:12	303.2056582	+0.2577355	2429	7.324	20	5
NGC 884	02:22:18	+57:08:12	141.2419556	-10.6452144	2345	7.032	18	5
NGC 957	02:33:21	+57:33:36	124.6487468	-13.4947336	1815	7.042	10	5
NGC 1513	04:09:57	+49:30:54	152.5898292	-1.5743179	1320	8.110	10	5
NGC 1528	04:15:23	+51:12:54	152.0568175	+0.2577355	776	8.568	16	5
Berkeley 11	04:20:36	+44:55:00	157.0814634	-3.6422252	2881	7.719	5	5
Berkeley 68	04:44:30	+42:04:00	162.1250204	-2.4076359	1678	8.391	12	5
NGC 1662	04:48:27	+10:56:12	187.6949501	-21.1142877	437	8.625	20	4
Berkeley 69	05:24:36	+32:39:00	174.4350179	-1.7867998	2860	8.950	3	5
Stock 8	05:27:36	+34:25:00	173.3194474	-0.2808586	1821	7.056	14	5
NGC 1960	05:36:18	+34:08:24	174.5344941	+1.0720022	1318	7.468	10	5
NGC 2099	05:52:18	+32:33:12	177.6353945	+3.0913643	1383	8.540	14	5
IC 2157	06:05:00	+24:00:00	186.4493104	+1.2519104	2040	7.800	5	5
Kharchenko 1	06:08:48	+24:19:54	186.5813745	+2.1705074	2520	0.000	7	5
NGC 2215	06:20:49	-07:17:00	215.9932108	-10.1024864	1293	8.369	7	2
Trumpler 5	06:36:42	+09:26:00	202.8646390	+1.0495276	3000	9.610	14	2
Collinder 110	06:38:24	+02:01:00	209.6491787	-1.9785548	1950	9.150	18	2
NGC 2264	06:40:58	+09:53:42	202.9357453	+2.1957346	667	6.954	39	1
NGC 2264(2)	06:40:58	+09:53:42	202.9357453	+2.1957346	667	6.954	39	2
NGC 2301	06:51:45	+00:27:36	212.5580952	+0.2791851	872	8.216	14	1
Berkeley 31	06:57:36	+08:16:00	206.2535550	+5.1198468	8272	9.313	5	2
NGC 2323	07:02:42	-08:23:00	221.6722021	-1.3311529	929	8.096	14	1
NGC 2354	07:14:10	-25:41:24	238.3683863	-6.7918076	4085	8.126	18	2
NGC 2353	07:14:30	-10:16:00	224.6853596	+0.3841506	1119	7.974	18	2
NGC 2374	07:23:56	-13:15:48	228.4146123	+1.0197776	1468	8.463	12	2
NGC 2423	07:37:06	-13:52:18	230.4835265	+3.5368466	766	8.867	12	2
NGC 2432	07:40:53	-19:04:36	235.4711964	+1.7782699	1905	8.800	6	1
NGC 2437	07:41:46	-14:48:36	231.8575777	+4.0644182	1375	8.390	20	2
NGC 2447	07:44:30	-23:51:24	240.0386236	+0.1345904	1037	8.588	10	2
NGC 2482	07:55:12	-24:15:30	241.6257467	+2.0345339	1343	8.604	10	1
NGC 2516	07:58:04	-60:45:12	273.8157504	-15.8558232	409	8.052	30	2
Haffner 21	08:01:09	-27:13:00	244.8500235	+1.6330592	2951	7.920	3	2
NGC 2527	08:04:58	-28:08:48	246.0873551	+1.8549763	601	8.649	10	2
NGC 2547	08:10:09	-49:12:54	264.4648854	-8.5974718	455	7.557	25	2
NGC 2539	08:10:37	-12:49:06	233.7053073	+11.1115046	1363	8.570	9	2
NGC 2546	08:12:15	-37:35:42	254.8551458	-1.9859258	919	7.874	70	1
NGC 2548	08:13:43	-05:45:00	227.8724676	+15.3928979	769	8.557	30	1
NGC 2567	08:18:32	-30:38:24	249.7950846	+2.9609760	1677	8.469	7	2
NGC 2579	08:20:52	-36:13:00	254.6741409	+0.2126247	1033	7.610	7	2
IC 2395	08:42:30	-48:09:00	266.6654791	-3.6144669	705	7.223	17	1
NGC 2670	08:45:30	-48:48:00	262.1476866	+0.7868650	1188	7.690	7	2
NGC 2669	08:46:22	-52:56:54	267.4854004	-3.6250419	1046	7.927	20	2
Trumpler 10	08:47:54	-42:27:00	262.7906250	+0.6740149	424	7.542	29	1
Collinder 205	09:00:32	-48:59:00	269.2091823	-1.8434708	1853	7.200	5	2
IC 2488	09:27:38	-57:00:00	277.8298005	-4.4192218	1134	8.113	18	1
Ruprecht 78	09:29:10	-53:42:00	275.7057596	-1.8814618	1641	7.987	3	2
NGC 2925	09:33:11	-53:23:54	274.6855749	+1.7570195	774	7.850	10	1
NGC 3228	10:21:22	-51:43:42	284.5638453	-0.3403225	544	7.932	5	1
IC 2581	10:27:29	-57:37:00	284.5879517	+0.0350265	2446	7.142	5	2
Trumpler 18	11:11:28	-60:40:00	290.9864152	-0.1346385	1358	7.194	5	2
NGC 3680	11:25:38	-43:14:36	124.9390350	-1.2226197	938	9.077	5	2
Ruprecht 98	11:58:40	-64:35:00	297.3059725	-2.2895622	494	8.508	14	1

Table 2: Cluster Basic Parameters (cont.)

Cluster	$\alpha_{2000.0}$	$\delta_{2000.0}$	l (°)	b (°)	d(pc)	Log(Age)	Diam(')	Run
Collinder 258	12:27:10	-60:46:00	299.9710726	+1.9654738	1184	8.032	5	1,2
NGC 5138	13:27:16	-59:02:00	307.7315236	+1.5616040	1986	7.986	7	2
Collinder 272	13:30:26	-61:19:00	307.5946828	+1.2015495	2045	7.227	10	2
NGC 5168	13:31:06	-60:56:24	309.1610046	-0.7137701	1777	8.001	4	2
NGC 5281	13:46:35	-62:55:00	309.0102495	-2.4915630	1108	7.146	7	2
NGC 5316	13:53:57	-61:52:06	311.6017200	+2.1144275	1215	8.202	14	2
Lynga 1	14:00:02	-62:09:00	310.8493823	-0.3373341	2283	8.007	3	2
NGC 5460	14:07:27	-48:20:36	316.3148289	+5.6067952	678	8.207	35	2
Lynga 2	14:24:35	-61:20:00	313.8642411	-0.4544184	1000	8.122	10	1
NGC 5617	14:29:44	-60:42:42	317.5264790	+2.0851683	1533	7.915	10	2
NGC 5662	14:35:37	-56:37:06	319.5288809	+4.5444922	666	7.968	29	1
NGC 5822	15:04:21	-54:23:48	324.3610672	+1.7201173	917	8.821	35	2
NGC 5823	15:05:30	-55:36:12	343.8165462	+19.8092470	1192	8.900	12	2
NGC 6031	16:07:35	-54:00:54	327.7257970	-5.4256670	1823	8.069	3	2
NGC 6067	16:13:11	-54:13:06	127.7404304	+2.0870193	1417	8.076	14	2
Harvard 10	16:18:48	-54:56:00	329.8356060	-3.2844232	1312	8.340	25	2
NGC 6124	16:25:20	-40:39:12	332.9179191	-3.1668043	512	8.147	39	1
NGC 6134	16:27:46	-49:09:06	335.2223160	-1.4272554	913	8.968	6	2
Ruprecht 119	16:28:15	-51:30:00	333.2758867	-1.8794014	956	6.853	8	1
NGC 6250	16:57:56	-45:56:12	341.9974370	-1.5166316	865	7.415	10	4
NGC 6259	17:00:45	-44:39:18	347.7305997	+1.9724630	1031	8.336	14	2
NGC 6281	17:04:41	-37:59:06	345.2791073	-3.0564946	479	8.497	8	2
NGC 6405	17:40:20	-32:15:12	356.9316398	-1.5491939	487	7.974	20	2
NGC 6416	17:44:19	-32:21:42	357.9402656	-1.6054677	741	8.087	14	2
NGC 6451	17:50:41	-30:12:36	6.5926834	-1.9594427	2080	8.134	7	2
NGC 6520	18:03:24	-27:53:18	355.7071381	-7.2997479	1577	7.724	5	4
NCG 6603	18:18:26	-18:24:24	15.8996436	+0.3505904	3600	8.300	6	2,3
IC 4756	18:39:00	+05:27:00	36.3807704	+5.2422154	484	8.699	39	4
NGC 6705	18:51:05	-06:16:12	15.3951139	-9.5927470	1877	8.302	13	4
NGC 6709	18:51:18	+10:19:06	42.8273977	+3.5653006	1075	8.178	14	3
NGC 6755	19:07:49	+04:16:00	39.9758453	-3.0034104	1421	7.719	14	4
NGC 6791	19:20:53	+37:46:18	40.0686817	-6.1221585	5853	9.643	10	5
NGC 6811	19:37:17	+46:23:18	73.9778116	8.4808440	1215	8.799	14	5
NGC 6834	19:52:12	+29:24:30	56.1143697	-5.1517479	2067	7.883	5	4
Roslund 3	19:58:42	+20:29:00	58.8105335	-4.6818307	1467	8.036	5	4
NGC 6866	20:03:55	+44:09:30	60.3897626	-6.0501422	1450	8.576	14	5
Roslund 4	20:04:54	+29:13:00	66.9839516	-1.2703113	2510	7.447	5	5
NGC 6871	20:05:59	+35:46:36	74.8979402	3.1181663	1574	6.958	29	5
Roslund 5	20:10:00	+33:46:00	71.4003205	+0.2729131	389	7.832	50	4
NGC 6885	20:11:58	+26:29:00	66.1352711	-6.3113024	597	9.160	10	4
IC 4996	20:16:30	+37:38:00	75.3533285	+1.3063273	1732	6.948	6	5
Berkeley 86	20:20:24	+38:42:00	76.6667475	+1.2725010	1112	7.116	6	5
NGC 6913	20:23:57	+38:30:30	95.9028469	+12.3043487	1148	7.111	10	5
NGC 7082	21:29:17	+47:07:36	94.4066042	+0.2199140	1442	8.233	25	5
Platais 1	21:30:02	+48:58:36	92.5613467	-1.6461398	1268	8.244	10	5
NGC 7209	22:05:07	+46:29:00	102.7010840	+0.7820237	1168	8.617	14	5
NGC 7654	23:24:48	+61:35:36	117.2878460	+10.8044002	1421	7.764	15	5

NOTES: Run 1: CTIO – Mar 2002, Run 2: CTIO – Mar 2003, Run 3: CTIO – Jul 2003, Run 4: CTIO – Aug 2003
Run 5: WIYN – Sep 2003,